

MicroMegascope

L Canale, A Laborieux, A Aroul Mogane, L Jubin, J Comtet, A Lainé,
L Bocquet, A Siria and A Niguès 

Laboratoire de Physique Statistique de l'École Normale Supérieure, UMR CNRS 8550, PSL Research University, 24 Rue Lhomond F-75005 Paris, France

E-mail: antoine.nigues@lps.ens.fr

Received 15 May 2018, revised 6 June 2018

Accepted for publication 11 June 2018

Published 21 June 2018



CrossMark

Abstract

Atomic force microscopy (AFM) allows us to reconstruct the topography of surfaces with resolution in the nanometer range. The exceptional resolution attainable with the AFM makes this instrument a key tool in nanoscience and technology. The core of a standard AFM set-up relies on the detection of the change of the mechanical motion of a micro-oscillator when approaching the sample to image. This is despite the fact that AFM is nowadays a very common instrument for both fundamental and applied research. The fabrication of the micrometric scale mechanical oscillator is still a very complicated and expensive task requiring dedicated platforms. Being able to perform AFM with a macroscopic oscillator would make the instrument more versatile and accessible for an even larger spectrum of applications and audience. Here, we present atomic force imaging with a centimetric oscillator, an aluminum tuning fork of centimeter size as a sensor on which an accelerometer is glued on one prong to measure the oscillations. We show that it is possible to perform topographic images of nanometric resolution with a gram tuning fork. In addition to the stunning sensitivity, we show the high versatility of such an oscillator by imaging both in air and liquid. The set-up proposed here can be extended to numerous experiments where the probe has to be heavy and/or very complex, and so too the environment.

Keywords: atomic force microscopy, instrumentation, tuning fork

(Some figures may appear in colour only in the online journal)

1. Introduction

The atomic force microscope (AFM) is a powerful instrument, which allows us to both reconstruct the topography of a sample surface and measure interactions at the nanoscale. Since its invention in 1986 by Binnig and Rohrer [1], much effort has been dedicated to this instrument to improve its capacities [2–4] and to make it affordable. Nowadays, AFM is an essential tool for a large spectrum of applications ranging from condensed matter and soft matter to biological science [5–7]. In the most commonly used configuration, a tiny mechanical oscillator, externally excited at the resonant frequency, is scanned over a surface; the interaction forces between a sharp tip at the apex of the oscillator and the sample induce a change in the mechanical properties of the oscillator itself. Keeping constant the interactions between the tip and surface during an image allows us then to reconstruct the sample topography with a resolution in the nanometer range. While the spatial resolution is only limited by the size of the tip, the ability to detect interaction forces relies

totally on the oscillator that is the force probe of the AFM. The standard and most common force probes are cantilevers with micro- and sub-micrometer dimensions. The quest for ultimate force sensitivities has pushed the development of alternative kinds of probes such as unidimensional objects such as nanowires and nanotubes and suspended membranes made of graphene and other 2D materials [8–12]. While the sensitivity is actually being pushed down to impressive values of zepto-Newton [13], these new probes present important constraints due to the challenges in the detection and working conditions and it is not possible to easily move them outside laboratory applications [14, 15]. On the other hand, and somehow in contrast to this, it is important to develop force probes that couple high sensitivities together with versatility; in this work, we present a new atomic sensor, named the MicroMegascope (MiMes), based on a centimetric harmonic oscillator. The advantages of using macroscopic probes is twofold: first, due to its dimensions, it is possible to change the specificity of the probe at convenience. This allows us then to study interactions in a variety of

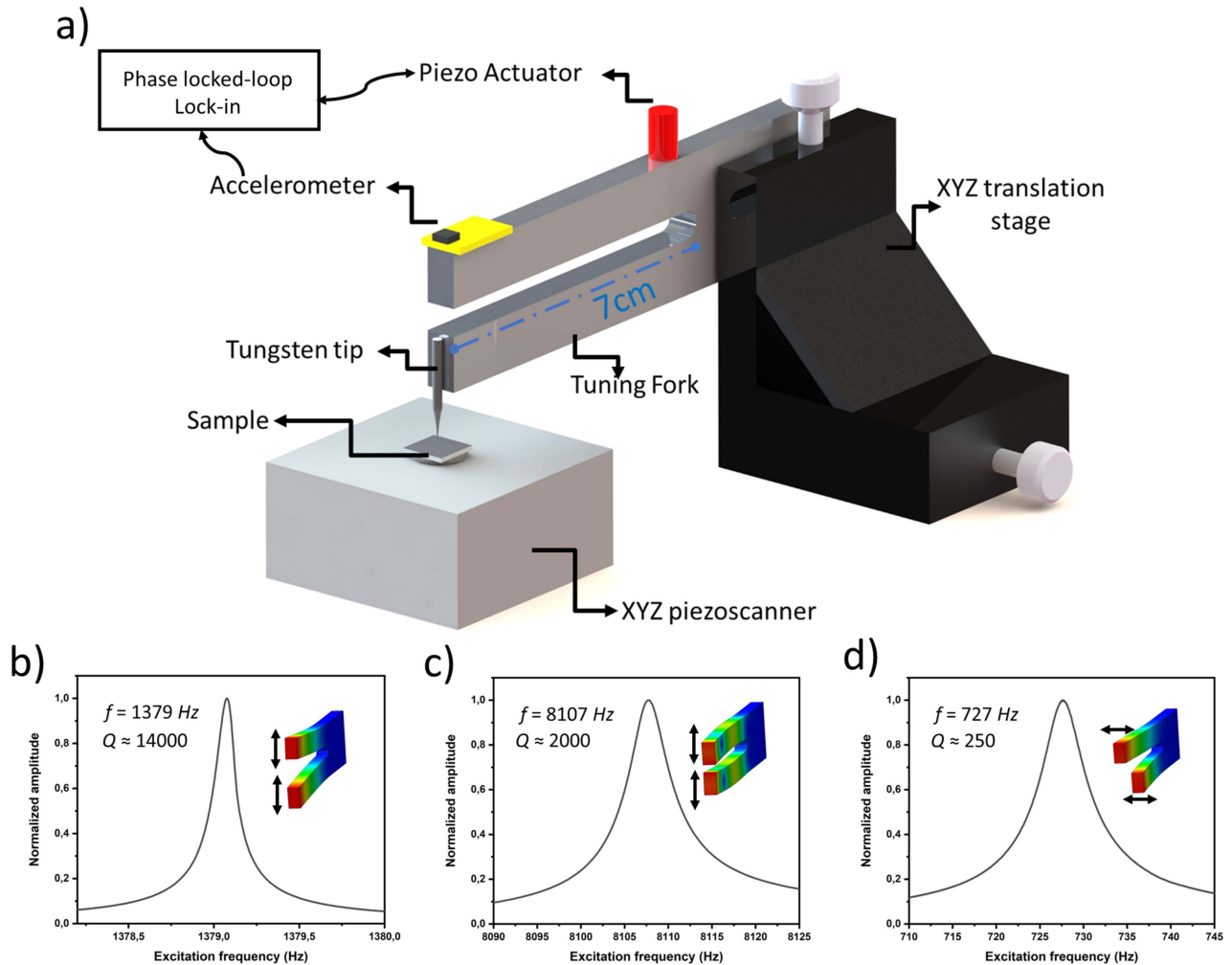


Figure 1. Experimental set-up and characterization. (a) Schematic drawing of the experimental set-up; a centimetric tuning fork to which a fine tungsten tip is attached is mechanically excited by a piezo at its resonant frequency. These oscillations are measured by an accelerometer glued to the end of one of the tuning fork arms. Signals from the accelerometer are transmitted to a lock-in and a phase-locked loop to keep both the amplitude and phase between the tuning fork and excitation constant. The tuning fork is attached to a translation stage for a coarse approach and a piezoscanner is used for a fine approach and nanoscale imaging of the sample. (b), (c) and (d) Resonance curve for, respectively, the fundamental and first harmonic of the normal mode and the fundamental harmonic of the tangential mode.

geometries ranging from nanometer size tips up to macroscopic spheres or more complex shapes ; second, due to its mass ($\approx 100\text{g}$) the coupling with macroscopic devices for position measurements does not affect the mechanical properties of the tuning fork enough to substantially decrease the force detection performances of the set-up. In addition to a study of the force detection performances of the MiMes and to demonstrate the potential of this new sensor, we perform in this work images at the nanoscale of a sample in air and totally immersed in a highly viscous liquid.

2. MiMes: experimental set-up and force sensor properties

The MiMes is presented in figure 1(a). The core of the microscope is a centimeter-sized tuning fork made of

aluminum. The tuning fork has been designed and realized to reproduce the same geometry and dimension ratio between the different elements as in quartz tuning forks widely used in AFM but with a rescaling factor of 20 [16]. The prong of the tuning fork is $l = 7.5\text{ cm}$ long, $w = 6, 8\text{ mm}$ wide and $t = 12\text{ mm}$ thick. The prong oscillations are detected using an accelerometer directly glued at the extremity of one prong. The oscillation amplitude A is directly proportional to the acceleration a_{acc} measured by the accelerometer so that $A = a_{\text{acc}}/f_0^2$. The tuning fork coupled to the accelerometer alone represents the MiMes. A similar device has been presented by Bosma *et al* [17], showing that the topography of a coin surface could be reconstructed with a resolution in the micron range. However, by increasing the mechanical properties of the force sensor and the displacement detection in the nanometer range, we can apply the technique to the field of AFM.

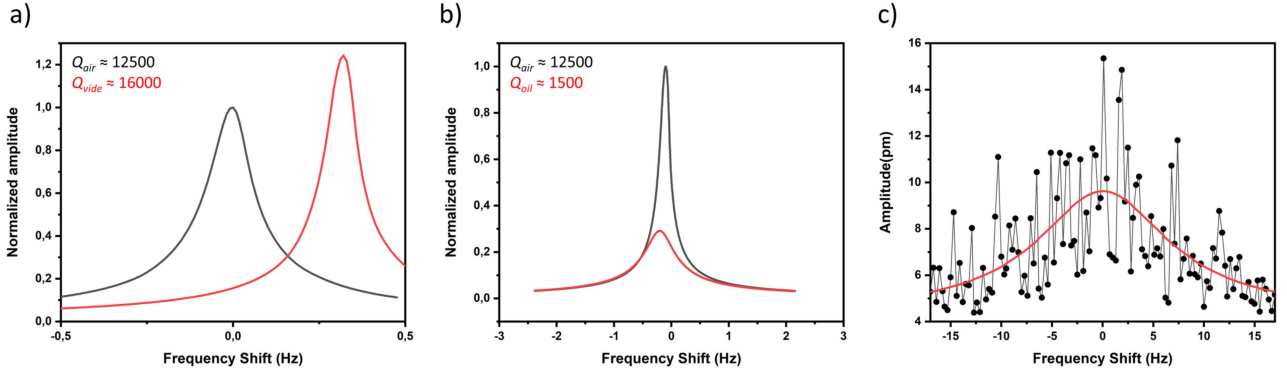


Figure 2. Mechanical response of the MiMes. (a) Resonance curves in air (black) and in vacuum (red). (b) Resonance curves in air (black) and with the tungsten tip immersed in highly viscous liquid (red). (c) Thermal noise of the MiMes detected through the accelerometer.

The tuning fork and its accelerometer are attached to an XYZ micrometric translation stage for the coarse approach. A piezo-actuator glued to the base of the tuning fork ensures the mechanical excitation. Furthermore, to perform images of sample surfaces, a chemically etched tungsten wire with a radius at the apex of ≈ 50 nm is glued at the extremity of one prong. Finally, the sample is placed on a three-axis piezo-scanner with sub-nanometric resolution in displacement (Tritor101 Piezosystemjena).

The spring constant k of the tuning fork is given by:

$$k = \frac{Ewt^3}{4l^3}, \quad (1)$$

where E is the Young's modulus for aluminum, $E = 69$ GPa leading to $k = 480$ kN m $^{-1}$. The resonance frequency of the fundamental mode is given by:

$$f_0 = \frac{\sqrt{k/m_{\text{eff}}}}{2\pi}, \quad (2)$$

where $m_{\text{eff}} = 0.24 \rho \times t \times w \times l = 3, 8$ g is the effective mass of that mode, $\rho = 2600$ kg m $^{-3}$ the mass density of aluminum. We then obtain $f_0 = 1788$ Hz. A finite element study enables us to test the mechanical parameters and characteristics of the tuning fork (inset figures 1(b)–(d)).

In figure 2, we show the mechanical response of the tuning fork around the fundamental resonant frequency. Despite its size, the macroscopic tuning fork is characterized by a low intrinsic dissipation and a large quality factor up to ≈ 12000 in air (figure 2(a)), allowing the detection of the oscillation amplitude of the tuning fork down to its thermal motion and to oscillation amplitudes of the order of 15 pm (figure 2(c)). It is worth comparing this value to the thermal variance expected for such a tuning fork, $\Delta x_{th}^2 = k_B T / m_{\text{eff}} \omega_0^2$, with k_B Boltzmann's constant and $T = 300$ K the ambient temperature. We find $\Delta x_{th}^2 = (10 \text{ pm})^2$, in very good agreement with the experimental value measured above.

At this point, it is now important to determine the force sensitivity of our tuning fork. The force sensitivity of an oscillator in a certain bandwidth B is given by [18]:

$$F_{\text{min}} = \sqrt{\frac{wt^2}{lQ}} (E\rho)^{(1/4)} (k_B TB)^{(1/2)}. \quad (3)$$

Inserting the parameters of the MiMes in equation (3) we obtain a minimal force detection of 21 pN/ $\sqrt{\text{Hz}}$. This minimum achievable force can be improved by a factor of one to two by improving the intrinsic dissipation of our tuning fork, by changing its manufacturing material and/or by working under vacuum conditions, as shown in figure 2(a). However, the force sensitivity obtained for the chosen configuration is already compatible with near-field force measurement and AFM.

The operating principle of a tuning fork as a force sensor is as follows: when excited by an external sinusoidal force $F_{\text{ext}}(\omega) = F_{\text{ext}} e^{i\omega t}$, the tuning fork behaves in first approximation as a spring-mass system with oscillation amplitude and phase with respect to the excitation given by:

$$A(\omega) = \frac{F_{\text{ext}}}{\sqrt{m_{\text{eff}}^2 (\omega_0^2 - \omega^2)^2 + \gamma^2 \omega^2}}, \quad (4)$$

$$\phi(\omega) = \arctan\left(\frac{\gamma\omega}{m_{\text{eff}}(\omega_0^2 - \omega^2)}\right), \quad (5)$$

with γ the damping factor. As the interaction of the oscillator with its environment is modified, one observes a change in both the frequency and amplitude at resonance. The shift in resonance frequency δf is related to the conservative force response, whereas the broadening of the resonance (change of quality factor $Q_0 \rightarrow Q_1$) is related to dissipation:

$$\frac{\partial F}{\partial r} = 2k \frac{\delta f}{f_0}, \quad (6)$$

$$F_D = \frac{kA}{\sqrt{3}} \left(\frac{1}{Q_0} - \frac{1}{Q_1} \right). \quad (7)$$

During the experiments, measurements and controls can be performed in real time by a complete Specs-Nanonis package (RT5, SC5 and OC4) and two feedback loops enable us to work at the resonance and maintain constant the oscillation amplitude A by changing the voltage amplitude applied to the piezo-actuator (figure 1(a)).

From equations (6) and (7), the ability to detect the interaction forces with a sample is determined by the spring constant of the force sensor and its Q factor. Even if the stiffness of the tuning fork is an order of magnitude larger than the classical quartz tuning fork and above the range of

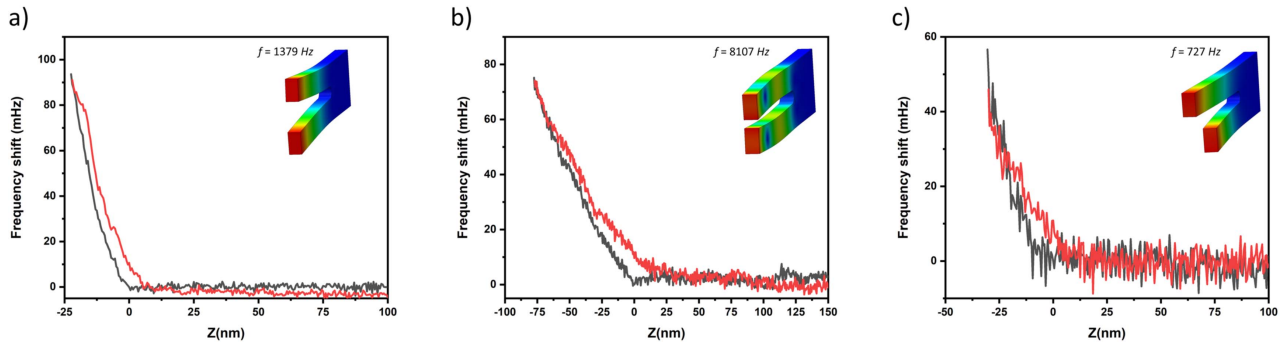


Figure 3. Force curves obtained with a tungsten tip on a silicon dioxide substrate at different frequencies: (a) Fundamental harmonics of normal mode (≈ 1350 Hz). (b) First harmonics of normal mode (≈ 8100 Hz). (c) Fundamental harmonics of the tangential mode (≈ 700 Hz). Approach in black, retract in red.

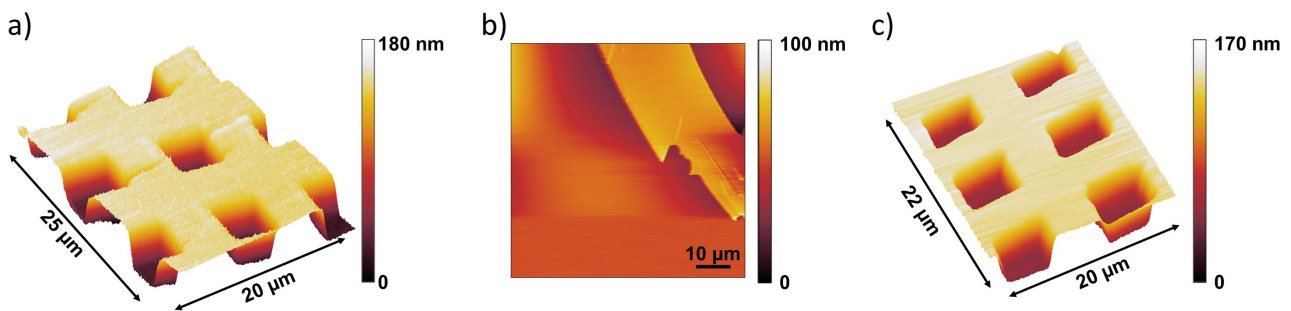


Figure 4. (a) Topographical image of calibration grating (pitch $5 \mu\text{m}$, depth 160 nm). (b) Topographical image of a mica surface. (c) Topographical image of the calibration grating immersed in silicon oil.

optimal stiffness values for frequency modulation microscopy [19, 17], we will show in the following that this is not a limiting factor for obtaining a nanometrically resolved image of the surface of a sample.

3. Results

To demonstrate the potential of MiMes for force microscopy we initially performed a series of approach-retract curves on a silicon dioxide flat surface. The interaction between the apex of a sharp tungsten tip glued at the extremity of one prong and the sample surface is detected by measuring the shift in the resonant frequency. In figure 3, we present the measurement for the fundamental frequency of the normal mode, the first harmonics of the same mode as well as the fundamental frequency of the tangential mode. These measurements prove that the macroscopic force sensor can detect the near-field interaction forces demonstrating that the technique can be applied to AFM applications and friction studies.

The AFM images in figure 4 have been performed in the so-called FM-AFM. In this mode the substrate is scanned with constant frequency shift, i.e. constant force gradient. The amplitude of vibration A of the tuning fork is kept constant at 10 nm . We present in figure 4 a nanometrically resolved standard calibration grating with a pitch of $5 \mu\text{m}$ and depth 180 nm (a) and the topographic image of a mica substrate (b).

Notwithstanding the effects inherent in the piezoelectricity of open-loop scanners (creep, hysteresis...), these first images obtained with a centimetric oscillator correspond in every aspect to the criteria expected with a conventional AFM probe. This irrefutably shows the exceptional sensitivity that our centimetric mechanical oscillator coupled with micro-electromechanical systems detection can achieve.

In order to push the nail even deeper and prove the great versatility of MiMes, we proceeded to the imaging of the same calibration grating as above, but completely immersed it in a highly viscous liquid, silicone oil (10000 cst). Indeed, it is no longer necessary to specify that AFM imaging in liquid media is still a challenge to this day. When fully immersed, the quality factor of conventional levers decreases drastically, laser detection is deteriorated by beam reflection on the liquid surface and multi-peak resonances appear making it difficult to distinguish the natural frequency of the lever. To tackle this problem with a conventional silicon cantilever, specific probes has been designed [20, 21]. Similar problems appear with quartz tuning forks. In our case, our sensor does not interact directly with the liquid, so its properties and sensitivity are not deteriorated. The image shown in figure 4(b) does not show any more defects than the one obtained in the air and its realization did not require more technical means than in the air. This completes the demonstration of the versatility, sensitivity and ease of use of the MiMes.

4. Conclusions and discussions

In conclusion, we have demonstrated that a macroscopic mechanical oscillator can be used as a force sensor for AFM. Despite the size and mass, the macroscopic tuning fork presents the force sensitivity needed to probe near-field surface interactions and image surface topography with nanometer resolution, provided a suitable tip is attached at the extremity of one prong. We have performed atomic force measurements and imaging in air and in a high viscous liquid, showing no remarkable effect of the environment on the image quality. Because of its size, the force sensor can support a macroscopic tip immersed in the fluid, while keeping the force sensor in the air, maintaining the mechanical properties and force sensitivity unperturbed.

It is worth citing that beyond the performance for AFM, centimeter-sized tuning forks can be implemented as force sensors for a broad spectrum of applications. The possibility to change the probe size and geometry, ranging from nanometric tips to macroscopic spheres, allows us to perform measurements of surface interactions in analogy with dynamical surface force apparatus [22]. Finally, the high mechanical stability and low intrinsic dissipation coupled with the possibility to detect orthogonal mechanical resonances, can open the way to the development of a new class of instruments for the measurement of friction phenomena in complex media [23].

ORCID iDs

A Niguès  <https://orcid.org/0000-0002-5818-4258>

References

- [1] Binnig J, Quate C F and Gerber C 1986 Atomic force microscope *Phys. Rev. Lett.* **56** 930–4
- [2] Giessibl F J 1995 Atomic resolution of the silicon (111)-(7x7) surface by atomic force microscopy *Science* **13** 68–70
- [3] Giessibl F J 2003 Advances in atomic force microscopy *Rev. Mod. Phys.* **3** 949–83
- [4] Extance A 2018 The atomic-force revolution *Nature* **555** 545
- [5] McGraw J, Niguès A, Chennevière A and Siria A 2017 Contact dependence and velocity crossover in friction between microscopic solid/solid contacts *Nano Lett.* **17** 6335–9
- [6] Comtet J, Niguès A, Kaiser V, Bocquet L and Siria A 2017 Nanoscale capillary freezing of ionic liquids confined between metallic interfaces and the role of electronic screening *Nat. Mater.* **16** 634–9
- [7] Dufrière Y F, Ando T, Garcia R, Alsteens D, Martinez-Martin D, Engel A and Müller D J 2017 Imaging modes of atomic force microscopy for application in molecular and cell biology *Nat. Nanotechnol.* **12** 295–307
- [8] Niguès A, Siria A and Verlot P 2015 Dynamical backaction cooling with free electrons *Nat. Commun.* **6** 8104
- [9] Gloppe A, Verlot P, Dupont-Ferrier E, Kuhn A G, Siria A, Poncharal P, Bachelier G, Vincent P and Arcizet O 2014 Bidimensional nano-optomechanics and topological backaction in a non-conservative radiation force field *Nat. Nanotechnol.* **9** 920–6
- [10] Poncharal P, Wang Z, Ugarte D and de Heer W A 1999 Electrostatic deflections and electromechanical resonances of carbon nanotubes *Science* **283** 1513–6
- [11] Miao T, Yeom S, Wang P, Standley B and Bockrath M 2014 Graphene nanoelectromechanical systems as stochastic-frequency oscillators *Nano Lett.* **6** 2982–7
- [12] De Alba R, Massel F, Storch I R, Abhilash T S, Hui A, McEuen P L, Craighead H G and Parpia J M 2016 Tunable phonon cavity coupling in graphene membranes *Nat. Nanotechnol.* **11** 741–6
- [13] Chaste J, Eichler A, Moser J, Ceballos G, Rurali R and Bachtold A 2012 A nanomechanical mass sensor with yoctogram resolution *Nat. Nanotechnol.* **5** 301–4
- [14] Siria A and Niguès A 2017 Electron beam detection of a nanotube scanning force microscope *Sci. Rep.* **7** 11595
- [15] Tsioutsios I, Tavernarakis A, Osmond J, Verlot P and Bachtold A 2017 Real-time measurement of nanotube resonator fluctuations in an electron microscope *Nano Lett.* **17** 1748–55
- [16] Karrai K and Grober R D 1995 Piezoelectric tip-sample distance control for near field optical microscopes *Appl. Phys. Lett.* **14** 1842–4
- [17] Bosma E, Offerhaus H L, Van Der Veen J T, Segerink F B and Van Wessel I M 2010 Large scale scanning probe microscope: making the shear-force scanning visible *Am. J. Phys.* **78** 562
- [18] Stowe T D, Yasumura K, Kenny T W, Botkin D, Wago K and Rugar D 1997 Attonewton force detection using ultrathin silicon cantilevers *Appl. Phys. Lett.* **71** 288–90
- [19] Giessibl F, Pielmeier F, Eguchi T, An T and Hasegawa Y 2011 Comparison of force sensors for atomic force microscopy based on quartz tuning forks and length-extensional resonators *Phys. Rev. B* **84** 1–15
- [20] Goertz M P and Moore N W 2010 Mechanics of soft interfaces studied with displacement-controlled scanning force microscopy *Prog. Surf. Sci.* **85** 347–97
- [21] Kim B I, Smith L, Tran T, Rossland S and Parkinson E 2013 Cantilever-based optical interfacial force microscope in liquid using an optical-fiber tip *AIP Adv.* **3** 032126
- [22] Restagno F, Crassous J, Charlaix É, Cottin-Bizonne C and Monchanin M 2002 A new surface forces apparatus for nanorheology *Rev. Sci. Instrum.* **73** 2292
- [23] Comtet J, Chatté G, Niguès A, Bocquet L, Siria A and Colin A 2017 Pairwise frictional profile between particles determines discontinuous shear thickening transition in non-colloidal suspensions *Nat. Commun.* **8** 15633